Computationally Efficient 2-step QRM-MLD for Single-Carrier Transmissions

Katsuhiro TEMMA† Tetsuya YAMAMOTO† and Fumiyuki ADACHI‡
Dept. of Electrical and Communication Engineering, Graduate School of Engineering, Tohoku University
6-6-05 Aza-Aoba, Aramaki, Aoba-ku, Sendai, 980-8579 Japan
E-mail: †{tenma, yamamoto}@mobile.ecei.tohoku.ac.jp, ‡adachi@ecei.tohoku.ac.jp

Abstract—**Recently, a frequency-domain block signal detection (FDBD) using maximum likelihood detection (MLD) employing QR decomposition and M-algorithm (QRM-MLD) was proposed for the reception of the single-carrier (SC) signals transmitted over a frequency-selective fading channel. SC-FDBD with QRM-MLD can significantly improve the bit error rate (BER) performance of SC transmission while reducing significantly the computational complexity compared to the MLD. However, its computational complexity is still high. In this paper, we propose a computationally efficient 2-step QRM-MLD SC-FDBD. Compared to conventional QRM-MLD, the number of symbol candidates can be reduced by using the decision made by minimum mean square error based frequency-domain equalization (MMSE-FDE). We evaluate the BER performance achievable by 2-step QRM-MLD and show that it can significantly reduce the computational complexity while keeping the BER performance almost the same as the conventional QRM-MLD.**

Keywords-component; Single-carrier, block signal detection, MMSE-FDE, QRM-MLD

I. INTRODUCTION

The broadband wireless channel is composed of many propagation paths with different time delays and therefore, characterized as a frequency-selective fading channel. In the frequency-selective fading channel, the bit error rate (BER) performance of single-carrier (SC) transmission severely degrades due to strong inter-symbol interference (ISI) [1]. Although the minimum mean square error based frequency-domain equalization (MMSE-FDE) can significantly improve the BER performance [2, 3], a big performance gap from the matched filter (MF) bound still exists due to presence of the residual ISI after FDE [4].

The optimum signal detection is maximum likelihood detection (MLD) [5]. However, MLD requires a prohibitively high computational complexity. Recently, the authors proposed a frequency-domain block signal detection (FDBD) using MLD employing QR decomposition and M-algorithm (QRM-MLD) [6] for the reception of the SC signals transmitted over a frequency-selective fading channel [7]. SC-FDBD with QRM-MLD can achieve the BER performance close to the MF bound by increasing the number of surviving paths [7], while requiring quite reduced complexity compared to MLD. However, its computational complexity is still high compared to MMSE-FDE.

In this paper, we introduce MMSE-FDE before performing QRM-MLD to limit the number of symbol candidates and hence, reduce the computational complexity of QRM-MLD. We call this proposed signal detection as 2-step QRM-MLD. We evaluate, by computer simulation, the average BER performance of SC transmissions achievable with 2-step QRM-MLD and compare it to conventional QRM-MLD.

The remainder of this paper is organized as follows. Sect. II presents the SC transmission with 2-step QRM-MLD. Sect. III, we evaluate by computer simulation the BER performance achievable with our proposed 2-step QRM-MLD and discuss how much we can reduce the number of symbol candidates. Sect. IV offers the conclusion.

II. 2-STEP QRM-MLD FOR SINGLE-CARRIER TRANSMISSIONS

A. SC Signal Representation

The SC transmission system model with 2-step QRM-MLD is illustrated in Fig. 1. Throughout the paper, the symbol-spaced discrete time representation is used. At the transmitter, a binary information sequence is data-modulated and then, the data-modulated symbol sequence is divided into a sequence of signal blocks of N_c symbols each, where N_c is the size of fast Fourier transform (FFT). The data symbol block is expressed using the vector form as $\mathbf{d}=[d(0), \ldots, d(N_c-1)]^T$. The last N_g symbols of each block are copied as a cyclic prefix (CP) and inserted into the guard interval (GI) placed at the beginning of each block and a CP-inserted data block of N_c+N_g symbols is transmitted.

We assume a symbol-spaced frequency-selective fading channel composed of L distinct propagation paths. The channel impulse response $h(\tau)$ is given by

$$h(\tau)=\sum_{l=0}^{L-1} h_l \delta(\tau-\tau_l), \tag{1}$$

where h_l and τ_l are respectively the complex-valued path gain with $E[\sum_{l=0}^{L-1}|h_l|^2]=1$ and the time delay of the lth path. The CP-removed received signal block $\mathbf{y}=[y(0), \ldots, y(N_c-1)]^T$ can be expressed using the vector form as

$$\mathbf{y}=\sqrt{\frac{2E_s}{T_s}}\mathbf{H}\mathbf{d}+\mathbf{n}, \tag{2}$$

where E_s and T_s are respectively the symbol energy and the symbol duration, $\mathbf{H}$ is the $N_c \times N_c$ channel impulse response matrix given as

978-1-4244-7006-8/10/$26.00 ©2010 IEEE

$$\mathbf{h}=\begin{bmatrix} h_0 & & & & & h_{L-1} & \cdots & h_1 \\ \vdots & h_0 & & & & & \ddots & \vdots \\ \vdots & \vdots & h_0 & & & \mathbf{0} & & h_{L-1} \\ h_{L-1} & \vdots & \vdots & \ddots & & & & \\ & h_{L-1} & \vdots & \ddots & h_0 & & & \\ & & h_{L-1} & \ddots & \vdots & \ddots & & \\ & \mathbf{0} & & \ddots & \vdots & \vdots & \ddots & \\ & & & & h_{L-1} & \cdots & \cdots & h_0 \end{bmatrix}, \quad (3)$$

and $\mathbf{n}=[n(0), \ldots, n(N_c-1)]^T$ is the noise vector whose element is the zero-mean additive white Gaussian noise (AWGN) having the variance $2N_0/T_s$ with N_0 being the one-sided noise power spectrum density each.

At the receiver, N_c-point FFT is applied to transform the received signal block into the frequency-domain signal vector $\mathbf{Y}=[Y(0), \ldots, Y(N_c-1)]^T$. $\mathbf{Y}$ is expressed as

$$\mathbf{Y}=\mathbf{Fy}=\sqrt{\frac{2E_s}{T_s}}\mathbf{Fhd}+\mathbf{N}, \quad (4)$$

where $\mathbf{N}=\mathbf{Fn}=[N(0), \ldots, N(N_c-1)]^T$ is the frequency-domain noise vector and $\mathbf{F}$ is the $N_c \times N_c$ FFT matrix given as

$$\mathbf{F}=\frac{1}{\sqrt{N_c}}\begin{bmatrix} 1 & 1 & \cdots & 1 \\ 1 & e^{-j2\pi\frac{1\times 1}{N_c}} & \cdots & e^{-j2\pi\frac{1\times(N_c-1)}{N_c}} \\ \vdots & \vdots & \ddots & \vdots \\ 1 & e^{-j2\pi\frac{(N_c-1)\times 1}{N_c}} & \cdots & e^{-j2\pi\frac{(N_c-1)\times(N_c-1)}{N_c}} \end{bmatrix}. \quad (5)$$

Due to the circulant property of $\mathbf{h}$ [8], we have

$$\mathbf{FhF}^H=diag\left[H(0),\cdots,H(N_c-1)\right]\equiv\mathbf{H}, \quad (6)$$

where $[.]^H$ is the Hermitian transpose operation and $H(k)=\sum_{l=0}^{L-1}h_l\exp(-j2\pi k\tau_l/N_c)$. Thus, Eq. (4) can be rewritten as

$$\mathbf{Y}=\sqrt{\frac{2E_s}{T_s}}\mathbf{FhF}^H\mathbf{Fd}+\mathbf{N}=\sqrt{\frac{2E_s}{T_s}}\mathbf{HFd}+\mathbf{N}=\sqrt{\frac{2E_s}{T_s}}\overline{\mathbf{H}}\mathbf{d}+\mathbf{N}. \quad (7)$$

By viewing a concatenation of propagation channel and FFT $\mathbf{HF}$ as an equivalent channel $\overline{\mathbf{H}}$, frequency-domain received SC signal can be treated as a received signal in MIMO multiplexing. According to this understanding, we apply MIMO detection scheme to SC block transmission.

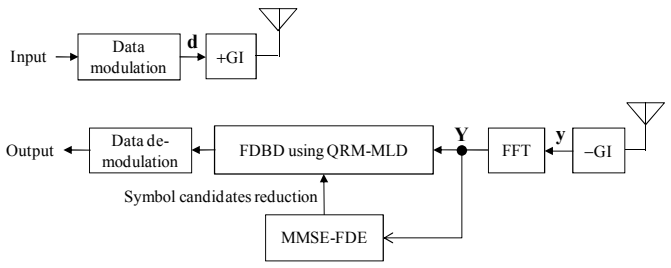

Figure 1. SC transmission with 2-step QRM-MLD system model.

B. Conventional QRM-MLD

SC-FDBD with QRM-MLD can significantly reduce the computational complexity compared to MLD. First, applying the QR decomposition to the equivalent channel matrix $\overline{\mathbf{H}}$, we have

$$\overline{\mathbf{H}}=\mathbf{QR}, \quad (8)$$

where $\mathbf{Q}$ is an $N_c \times N_c$ unitary matrix and $\mathbf{R}$ is an $N_c \times N_c$ upper triangular matrix. Then, multiplexing $\mathbf{Y}$ by $\mathbf{Q}^H$, the transformed frequency-domain received signal $\mathbf{Z}$ is obtained as

$$\mathbf{Z}=\left[Z(0),\cdots,Z(N_c-1)\right]^T=\mathbf{Q}^H\mathbf{Y}=\sqrt{\frac{2E_s}{T_s}}\mathbf{Rd}+\hat{\mathbf{N}}$$
$$=\sqrt{\frac{2E_s}{T_s}}\begin{bmatrix} R_{0,0} & R_{0,1} & \cdots & R_{0,N_c-1} \\ & R_{1,1} & \cdots & R_{1,N_c-1} \\ & & \ddots & \vdots \\ \mathbf{0} & & & R_{N_c-1,N_c-1} \end{bmatrix}\begin{bmatrix} d(0) \\ d(1) \\ \vdots \\ d(N_c-1) \end{bmatrix}+\hat{\mathbf{N}}. \quad (9)$$

From Eq. (9), the MLD is represented as

$$\hat{\mathbf{d}}=\underset{\bar{\mathbf{d}}\in X^{N_c}}{\arg\min}\left(\sum_{i=0}^{N_c-1}\left|Z(N_c-1-i)-\sum_{j=0}^{i}\sqrt{\frac{2E_s}{T_s}}R_{N_c-1-i,N_c-1-j}\bar{d}(N_c-1-j)\right|^2\right), \quad (10)$$

where $\bar{\mathbf{d}}=[\bar{d}(0),\ldots,\bar{d}(N_c-1)]^T$ is the symbol candidate vector and X is the modulation level (X=4 for QPSK and X=16 for 16QAM).

M-algorithm [9] is composed of N_c stages, each stage for detecting one of N_c symbols in a block. In ith stage (i=0~N_c–1), path metric based on the squared Euclidean distance between the transformed frequency-domain received signal $Z(N_c-1-i)$ and the symbol candidates $\bar{d}(N_c-1) \sim \bar{d}(N_c-1-i)$ is calculated. The accumulated path metric, which is the sum of path metric at the present stage and the accumulated path metric at the previous stage, is updated. Then best M paths are selected by comparing the accumulated path metrics associated with all surviving paths at the present stage. This process is repeated until the last stage. The most possible transmitted symbol sequence is found by tracing back staring from the best surviving path having the smallest accumulated path metric at the last stage (i=N_c–1). By using M-algorithm, the number of path metric computations is reduced from $\sum_{n=1}^{N_c}X^n$, which is required for full MLD, to $X\{1+M(N_c-1)\}$.

C. 2-step QRM-MLD

The complexity of path metric calculation in the SC-FDBD with QRM-MLD depends on the block size N_c, the number M of surviving paths at each stage and the number N_{cand} of candidate symbols for metric computation. Recently, we have proposed the method of reduction M [10, 11]. In this paper, we want to reduce N_{cand}. The proposed scheme is called 2-step QRM-MLD.

In conventional QRM-MLD, the path metric is calculated for all symbol candidates at each stage (i.e., N_{cand}=X) in order to decide the likelihood of each symbol candidate. In 2-step QRM-MLD, MMSE-FDE is performed prior to QRM-MLD to

limit the value of N_{cand} and then, to discard the symbol candidates having low reliability at each stage.

In the first step, MMSE-FDE is carried out by multiplying the frequency-domain received signal **Y** by MMSE weight matrix **W** [3] as

$$\hat{\mathbf{Y}} = \mathbf{WY}, \tag{11}$$

where

$$\mathbf{Y} = \sqrt{\frac{2E_s}{T_s}}\mathbf{Fhd} + \mathbf{N} = \sqrt{\frac{2E_s}{T_s}}\mathbf{FhF}^H\mathbf{Fd} + \mathbf{N} = \sqrt{\frac{2E_s}{T_s}}\mathbf{HD} + \mathbf{N}, \tag{12}$$

$$\mathbf{W} = diag\left[\frac{H^*(0)}{|H(0)|^2 + \left(E_s/N_0\right)^{-1}}, \cdots, \frac{H^*(N_c-1)}{|H(N_c-1)|^2 + \left(E_s/N_0\right)^{-1}}\right], \tag{13}$$

D is the frequency-domain transmitted signal vector and $[.]^*$ denotes of the conjugate operation. Then, applying N_c-point inverse FFT (IFFT) to $\hat{\mathbf{Y}}$, the time-domain received symbol vector $\hat{\mathbf{y}}$ is obtained as

$$\hat{\mathbf{y}} = \mathbf{F}^H\hat{\mathbf{Y}}. \tag{14}$$

Finally, the hard detection is done on $\hat{\mathbf{y}}$.

In the second step, QRM-MLD is carried out. The symbol candidates having the same Euclidean distance from the hard detection result of MMSE-FDE have the same reliability. Therefore, in 2-step QRM-MLD, the symbol candidates are limited within the distance r from the hard detection result of MMSE-FDE. Figure 2 shows an example of the symbol candidate limitation in 16QAM case. In this way, the computational complexity can be further reduced by reducing the value of r. However, the use of too small r leads to the BER performance degradation. Therefore, the optimum r exists.

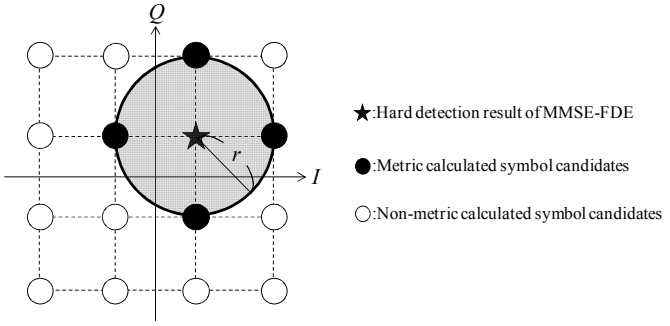

Figure 2. An example of the symbol candidates limitation (16QAM).

III. COMPUTER SIMULATION

First, we find the optimum r. Then, we show the BER performance of 2-step QRM-MLD and compare it with the conventional QRM-MLD. The computer simulation condition is shown in Table I. We assume QPSK and 16QAM data modulation, block size N_c=64, and GI size N_g=16. The channel is assumed to be a frequency-selective block Rayleigh fading channel having symbol-spaced L=16-path uniform power delay profile. Ideal channel estimation is assumed.

TABLE I. COMPUTER SIMULATION CONDISION

Transmitter	Modulation	QPSK, 16QAM
	Block size	N_c=64
	GI	N_g=16
Channel	Fading type	Frequency-selective block Rayleigh
	Power delay profile	L=16-path uniform power delay profile
	Time delay	τ_l=l(l=0~L–1)
Receiver	Channel estimation	Ideal
	Detection	MMSE-FDE, QRM-MLD, 2-step QRM-MLD

A. Optimization of r

In order to find the optimum r, we measure the *a posteriori* probability distribution of transmitted symbol candidates when the hard detection result of MMSE-FDE is given. As shown in Fig. 3, since the signal constellation is circularly symmetric, it is sufficient to measure the *a posteriori* probability distribution of symbol candidates for detected symbols falling in the first quadrant.

The *a posteriori* probability distribution obtained by the computer simulation is shown in Figs. 4 and 5. It can be seen from Fig. 4 that the *a posteriori* probability of the most distant symbol candidate (No. 3) is quite low in QPSK case, so we can set $r = \sqrt{2}$ as shown in Fig. 6(a). In 16QAM case, it is seen from Fig. 5 that the *a posteriori* probability of the symbols located outside a circle with the radius $2/\sqrt{5}$ in the Euclidean distance from the hard detection result of MMSE-FDE is negligible. Therefore, we can set $r = 2/\sqrt{5}$. In this paper, for comparison, we also evaluate the BER performances of 2-step QRM-MLD with $r = 2/\sqrt{10}$ and $4/\sqrt{10}$ as shown in Fig. 6(b).

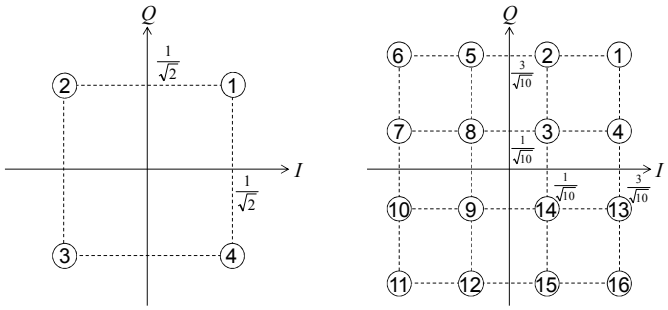

(a) QPSK (b) 16QAM

Figure 3. Constellation diagram.

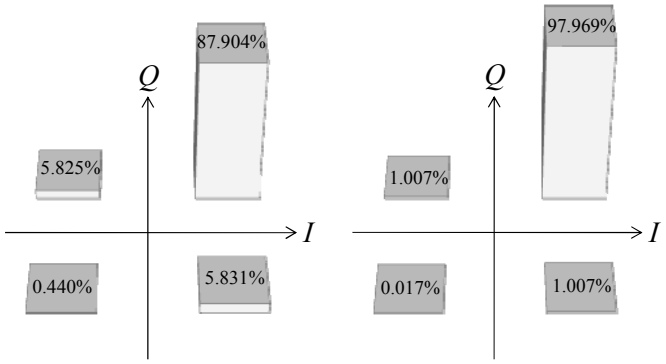

(a) Average Received E_b/N_0=5dB (b) Average Received E_b/N_0=10dB

Figure 4. *A posteriori* probability distribution (QPSK).

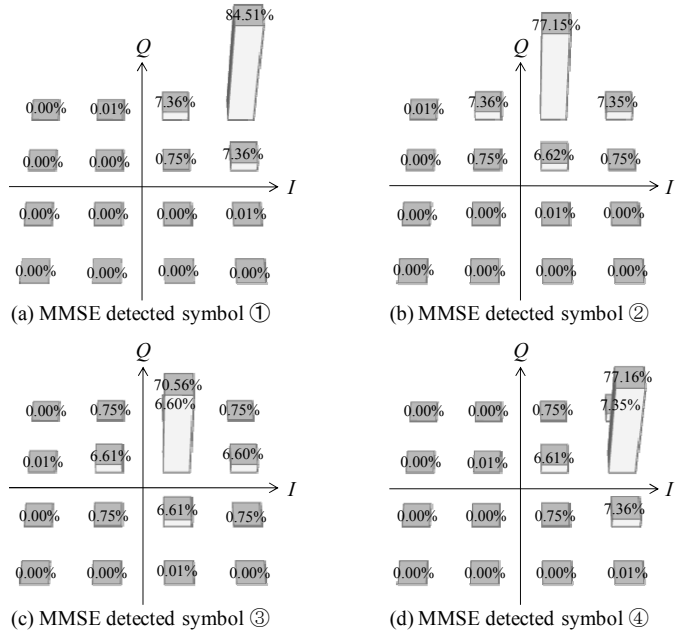

(a) MMSE detected symbol ① (b) MMSE detected symbol ②

(c) MMSE detected symbol ③ (d) MMSE detected symbol ④

Figure 5. *A posteriori* probability distribution of transmitted symbol candidates (16QAM, Average Received E_b/N_0=10dB).

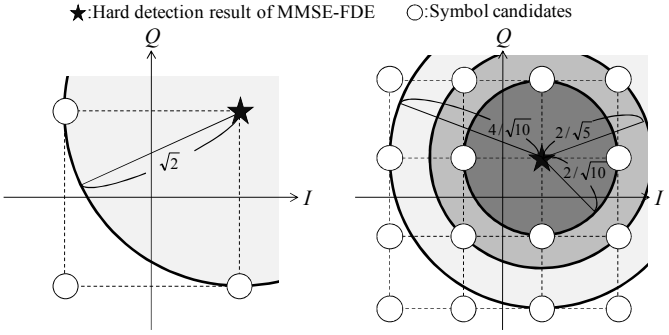

(a) QPSK (b) 16QAM

Figure 6. Symbol candidate selection.

B. BER performance & Computational complexity

The average BER performance of 2-step QRM-MLD assuming 16QAM with $r = 2/\sqrt{10}$, $2/\sqrt{5}$ and $4/\sqrt{10}$ is plotted in Fig. 7 as a function of the average received bit energy-to-noise power spectrum density ratio E_b/N_0 ($=(E_s/N_0)(1+N_c/N_g)/\log_2 X$). When the number of survival paths M=16, almost the same BER performance is achieved. However, when M=256, the BER performance in the case of $r = 2/\sqrt{10}$ is inferior to others. This is because the correct symbol candidates are likely discarded since $r = 2/\sqrt{10}$ is relatively small. Therefore, from the viewpoint of the computational complexity reduction, the optimum r is $2/\sqrt{5}$ for 16QAM case.

Figure 8 compares the BER performances of 2-step QRM-MLD and conventional QRM-MLD. Three cases of the number M of surviving paths in M-algorithm are plotted, i.e., M=4, 16, and 64 for QPSK and M=16, 64, and 256 for 16QAM. Also plotted for comparisons are the MF bound [12] and the average BER performance of MMSE-FDE. In 2-step QRM-MLD, r is set to $\sqrt{2}$ for QPSK and $2/\sqrt{5}$ for 16QAM. In QPSK with M=4 and 16QAM with M=16 case, the BER performance of 2-step QRM-MLD is better than that of conventional QRM-MLD. This is because the paths with low reliability are pruned in the first step and therefore, the probability to select an incorrect path is lower than the conventional QRM-MLD. However, when the value of M is increased to 64, the BER performance of 2-step QRM-MLD is almost the same as the conventional QRM-MLD in 16QAM case while it is slightly degraded in QPSK case. This performance degradation is due to the effect of symbol candidate limitation.

The computational complexity of the SC transmissions with 2-step QRM-MLD, in terms of the number of complex multiply operations, is compared with those of the SC transmission with conventional QRM-MLD and MMSE-FDE. In Table II, the computational complexity is shown. 2-step QRM-MLD can reduce the number of path metric calculations compared to the conventional QRM-MLD. The complexity for the path metric calculation is $N_{cand}\times\{2+(M/2)(N_c+4)(N_c-1)\}$, where N_{cand} is the number of candidate symbols and is 4 for QPSK and 16 for 16QAM for conventional QRM-MLD. However, in 2-step QRM-MLD, N_{cand} can be reduced to 3 for QPSK and 6.25 (which is the average when all the symbols are transmitted with the same probability) for 16QAM. Hence, 2-step QRM-MLD can reduce the total amount of computational complexity to about 83(41)% of the conventional QRM-MLD in M=64(256) case when QPSK(16QAM) is used.

TABLE II. NUMBER OF COMPLEX MULTIPLY OPERATIONS

	MMSE-FDE	QRM-MLD	2-step QRM-MLD
FFT	$N_c\log_2 N_c$	$N_c\log_2 N_c$	$N_c\log_2 N_c$
MMSE-weight calc. & FDE	N_c+N_c		N_c+N_c
IFFT	$N_c\log_2 N_c$		$N_c\log_2 N_c$
HF calc. & QR decomposition		$N_c^2+N_c^3$	$N_c^2+N_c^3$
Multiplication of $\mathbf{Q}^H$		N_c^2	N_c^2
Path metric calc.		$N_{cand}\times\{2+(M/2)(N_c+4)(N_c-1)\}$; N_{cand}=4(16) for QPSK(16QAM)	$N_{cand}\times\{2+(M/2)(N_c+4)(N_c-1)\}$; N_{cand}=3(6.25) for QPSK(16QAM)

IV. CONCLUSION

In this paper, we proposed the computationally efficient 2-step QRM-MLD that utilizes MMSE-FDE prior to QRM-MLD in order to reduce the number of symbol candidates for metric calculation. The symbol candidates outside a circle of the radius r from the hard detection of MMSE-FDE are discarded. We discussed the *a posteriori* probability distribution of transmitted symbols when the hard detection result of MMSE-FDE is given and optimized the value of r. We showed that 2-step QRM-MLD can achieve almost the same BER performance as the conventional QRM-MLD while reducing the computational complexity to about 41% of the conventional QRM-MLD for 16QAM.

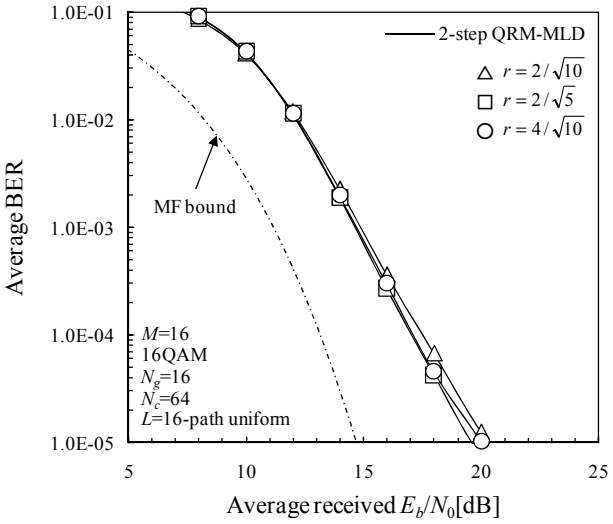

(a) M=16

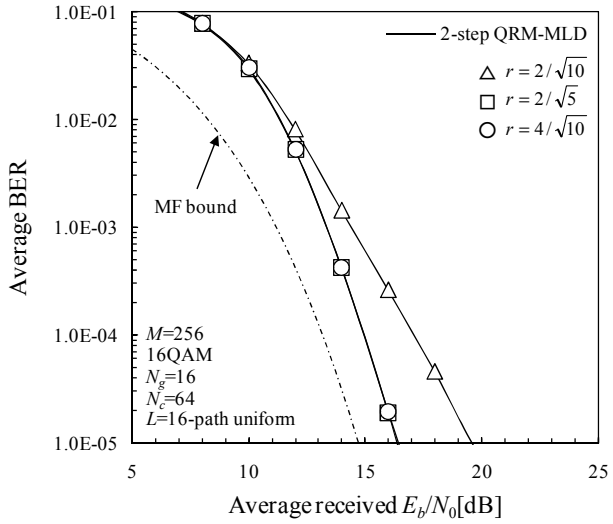

(b) M=256

Figure 7. BER performance of 2-step QRM-MLD for 16QAM.

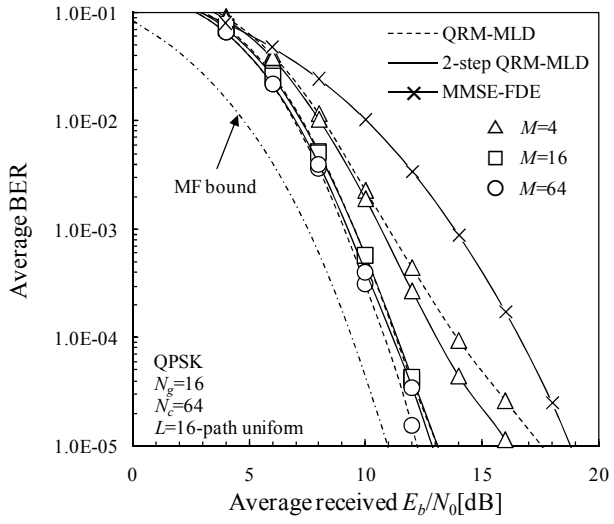

(a) QPSK

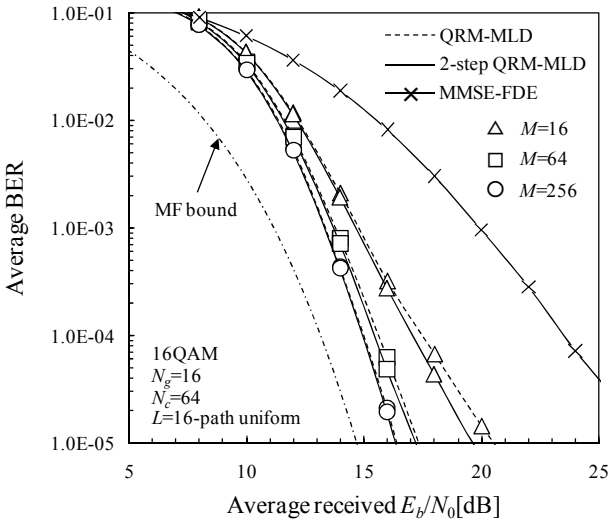

(b) 16QAM

Figure 8. BER performance-comparison between 2-step QRM-MLD and the conventional QRM-MLD.

REFERENCES

[1] J. G. Proakis and M. Salehi, *Digital communications*, 5th ed., McGraw-Hill, 2008.

[2] D. Falconer, S. L. Ariyavisitakul, A. Benyamin- Seeyar and B. Edison, "Frequency domain equalization for single-carrier broadband wireless systems," IEEE Commun. Mag., Vol. 40, No. 4, pp. 58-66, Apr. 2002.

[3] K. Takeda, T. Itagaki and F. Adachi, "Joint use of frequency-domain equalization and transmit/receive antenna diversity for single-carrier transmissions," IEICE Trans. Commun., Vol. E87-B, No. 7, pp.1946-1953, Jul. 2004.

[4] K. Takeda, K. Ishihara and F. Adachi, "Frequency-domain ICI cancellation with MMSE equalization for DS-CDMA downlink," IEICE Trans. Commun., Vol. E89-B, No. 12, pp. 3335-3343, Dec. 2006.

[5] A. van Zelst, R. van Nee and G. A. Awater, "Space division multiplexing (SDM) for OFDM systems," IEEE VTC2000-Spring, pp. 1070-1074, May 2000.

[6] L. J. Kim and J. Yue, "Joint channel estimation and data detection algorithms for MIMO-OFDM systems," in Proc. Thirty-Sixth Asilomar Conference on Signals, System and Computers, pp. 1857-1861, Nov. 2002.

[7] T. Yamamoto, K. Takeda and F. Adachi, "Single-carrier transmission using QRM-MLD with antenna diversity," The 12th International Symposium on Wireless Personal Multimedia Communications (WPMC 2009), Sendai, Japan, Sept. 2009.

[8] G. H. Golub and C. F. van Loan, *Matrix Computations*, 3rd ed. Baltimore, MD, Johns Hopkins Univ. Press, 1996.

[9] J. B. Anderson and S. Mohan, "Sequential coding algorithms: A survey and cost analysis," IEEE Trans. on Commun., Vol. 32, pp. 169-176, Feb. 1984.

[10] T. Yamamoto, K. Takeda, and F. Adachi, "Training sequence aided single-carrier block signal detection using QRM-MLD," IEEE Wireless Communication & Networking Conference (WCNC), Apr. 2010.

[11] T. Yamamoto, K. Takeda, and F. Adachi, "MMSE based QRM-MLD Frequency-domain block signal detection for single-carrier transmission," The 7th IEEE VTS Asia Pacific Wireless Communication Symposium (APWCS 2010), Taiwan, May 2010

[12] F. Adachi and K. Takeda, "Bit error rate analysis of DS-CDMA with joint frequency-domain equalization and antenna diversity combining," IEICE Trans. Commun., Vol. E87-B, No. 10, pp.2991-3002, Oct. 2004